Catalysis Today 155 (2010) 319–325

Contents lists available at ScienceDirect

Catalysis Today

journal homepage: www.elsevier.com/locate/cattod

Persistent species formed during the carbon dioxide reforming of methane over a nickel–alumina catalyst

Ian P. Silverwood[a], Neil G. Hamilton[a], John Z. Staniforth[b], Christian J. Laycock[b], Stewart F. Parker[c], R. Mark Ormerod[b], David Lennon[a,*]

[a] Department of Chemistry, Joseph Black Building, The University of Glasgow, Glasgow, G12 8QQ, Scotland, UK
[b] School of Physical & Geographical Sciences, Keele University, Staffs, ST5 5BG, UK
[c] ISIS Facility, Rutherford Appleton Laboratory, Chilton, Didcot, Oxon, OX11 0QX, UK

ARTICLE INFO

Article history:
Available online 21 August 2010

Keywords:
Methane reforming
Inelastic neutron scattering
Vibrational spectroscopy
Nickel–alumina catalyst

ABSTRACT

The CO_2 reforming of methane over an alumina-supported nickel catalyst has been studied using a conventional micro-reactor set-up. These experiments have been used to guide inelastic neutron scattering (INS) measurements, which were performed post-reaction using a 'quench' technique. The reacted catalyst has also been examined using infrared spectroscopy and transmission electron microscopy. This unified approach reveals the presence of a hydrogen-lean coke to have formed during the reforming process, which is predominantly comprised of amorphous carbon, the domains of which appear to be terminated with a small number of hydrocarbon groupings. A semi-quantitative analysis of the INS spectra establishes the catalyst to be very effective in cycling hydrogen during the reforming process.

1. Introduction

As oil reserves have dwindled and the price of oil has shown great variability, interest in methane both as a fuel and as a chemical feedstock has increased significantly. To exploit methane in this manner, production of synthesis gas is a key requirement. Commercially, steam is most frequently used as the oxidant in the steam reforming reaction ($CH_4 + H_2O \rightarrow CO + 3H_2$), although this has high energy requirements. The alternative use of CO_2 as the methane oxidant is well known, and has the obvious potential benefit of consuming greenhouse gases. This "dry-reforming" reaction is also endothermic, although it requires less energy than the steam reforming reaction when the steam is generated through vaporisation of water. In addition, the H_2:CO ratio in the synthesis gas produced *via* the dry-reforming reaction (~1:1) is more suited to Fischer–Tropsch synthesis, allowing the production of higher hydrocarbons from a linked plant [1]. Nickel catalysts are most commonly used but a particular limitation is their susceptibility to coking which results in catalyst deactivation [1–3]. Although noble metals may show higher activities and less coke deposition, their high costs rarely justify their use [4]. Various forms of carbon are known and characterised [5]. Highly reactive monatomic carbon is formed on the nickel surface during reaction, commonly denoted as C_α or surface carbide. This can react to form gaseous species, dissolve in the nickel to form a bulk carbide (C_γ), or polymerise to an amorphous carbon, C_β. As the reaction continues, dissolved carbon is likely to precipitate out of the nickel particle as a filament, which may be either amorphous or graphitic. This process can cause considerable mechanical damage to the catalyst, and cause pressure to build up, without significant deactivation [6]. At higher temperatures, encapsulating crystalline graphite (C_c) may form upon the nickel surface, preventing access to the metal by the reactants and thus the catalytic reaction ceases. Although recently carbon filament growth has been well characterised under certain conditions [7,8], the inter-conversion of the other carbon species and their precise morphology is still elusive. Key to the understanding of such materials is the relative amount of sp^2 and sp^3 hybridised carbon [9] and the role of polycyclic aromatic hydrocarbons [10], which have been identified in various cokes. The aim of this work was to bring a fresh perspective to the field through the use of vibrational spectroscopy to characterise the materials left upon the catalyst surface after continued reaction. This is a challenging matter due to the difficulty in gaining optical spectra from these highly absorbing materials. With care, however, it is possible to gain adequate optical measurements from such dark samples, as shown previously [11,12]. In addition, inelastic neutron scattering (INS) is a non-optical method that also provides vibrational information and has proved its use in determining the interaction of adsorbates with catalysts [13–16] and other optically challenging materials [9,17,18]. Furthermore, infrared spectroscopy of supported metal catalysts is often hindered by strong absorptions from the support material (e.g. ν(Si–O) for silica or ν(Al–O) for alumina) that

* Corresponding author. Tel.: +44 0141 330 4372; fax: +44 0141 330 4888.
E-mail address: d.lennon@chem.gla.ac.uk (D. Lennon).

0920-5861/$ – see front matter © 2010 Elsevier B.V. All rights reserved.
doi:10.1016/j.cattod.2010.07.009

effectively define a 'cut-off' region (<1300 and <1100 cm^{-1}, respectively) [19]. Due to the low neutron scattering cross-section for these oxides, this important region of the vibrational spectrum is accessible to INS.

This work uses micro-reactor studies to define the operational characteristics for the Ni/Al_2O_3 catalyst under investigation, which is representative of methane reforming catalysts [20]. Those studies have then guided isothermal conditions that were used for the INS measurements. Due to the relative insensitivity of the INS technique [21], a scale up factor of *ca.* 10^3 was required on going from the micro-reactor operation (*ca.* 20 mg of catalyst) to the INS operation (*ca.* 20 g of catalyst). Nevertheless, temperature-programmed oxidation experiments indicate that the carbonaceous layer formed during the micro-reactor and INS studies is of a comparable nature. Although this work does not strictly adopt *operando* principles, it outlines a methodology that permits INS measurements of the active phase of commercially relevant supported metal catalysts to be probed over a wider dynamic range than that accessible using infrared spectroscopy. Moreover, semi-quantitative analysis of the resulting INS spectra is used to evaluate the extent to which hydrogen is incorporated in to the important carbonaceous overlayer.

2. Experimental

2.1. Catalyst preparation and reaction testing

The catalyst sample was prepared by wet impregnation of α-alumina with nickel nitrate (Alfa, 99.9%) followed by calcination at 900 °C. A known quantity of nickel nitrate hexahydrate was dissolved in a minimal amount of water to which alumina was then added. Water was driven off the suspension using a hot plate, before drying in an oven at 120 °C for 6 days. Finally, the material was calcined in static air by heating to 500 °C at 1 °C min^{-1}, then to 900 °C at 5 °C min^{-1}. The temperature was maintained for 1 h before cooling to room temperature at 10 °C min^{-1}. This provided a 26% (w/w) Ni/Al_2O_3 catalyst. Reaction testing was carried out in a quartz-tube micro-reactor attached to a previously described flow system [22]. All catalyst test experiments [temperature-programmed reduction (TPR), temperature-programmed reaction (TPRxn), isothermal reforming and temperature-programmed oxidation (TPO)] were performed at least in duplicate, with the results presented here being representative of the multiple datasets. Typically a catalyst mass of *ca.* 20 mg was used for these measurements with the reactor operating at a gas hourly space velocity (GHSV) of 54,000 $cm^3/(g_{cat}\ h)$ and a mean contact time of 3.5×10^{-4} min. During these micro-reactor measurements a sharp 'spike' in the partial pressures of the reacting gases was observed at the commencement of reaction. This abrupt feature is associated with the catalyst switching over from a passive to an active regime; thereafter reaction profiles are more gradual. Measurements were continued above this activation point to establish steady-state or near steady-state operation.

2.2. Reaction testing arrangements for INS measurements

The INS technique is primarily sensitive to hydrogen, due to its uniquely high neutron scattering cross-section. In order to observe the minority adsorbed species upon an inorganic catalyst, a large sample is needed to obtain an acceptable level of hydrogenous material. A gas handling system capable of treating this volume of material for extended periods under reaction conditions was therefore commissioned. The system comprises a gas supply and mixing stage, U-tube reactor and an effluent monitoring system. 1/4 in. stainless steel tubing and Swagelok connectors were used for connections throughout. For gas supply three 0–100 ml N_2 min^{-1} rotameters (Platon) were used to control flows of H_2, CO_2 and CH_4. One 2 l N_2 min^{-1} rotameter controlled the flow of He diluent. The outlets from the flowmeters were joined through union fittings and directed through a short length of 1 in. diameter tube filled with Ballotini glass spheres to ensure a homogeneous gas phase entered the reactor.

The reactor design took the form of two 3/4 in. tubes connected using reducing unions and a 1/4 in. tube bent into a U-shape. Spot welded wire gauzes at the lower end of the large tubes provided supports to hold quartz Raschig rings on the inlet and the catalyst on the outlet. The inlet arm was designed to pre-heat the gas before encountering the catalyst and the Raschig rings were used to ensure a convoluted flow path to achieve this objective. Shut-off valves were placed immediately above the reactor allowing the sample to be isolated under helium after reaction. The reactor was held inside a bucket furnace (Instron) attached to a temperature controller (Eurotherm), with a quartz wool plug inserted to minimise heat loss due to convection.

To monitor the reaction progress, the effluent gases were followed with a quadrupole mass spectrometer (MKS Instruments). This was connected to the exhaust line via a needle valve, which was used to control the flow into the instrument.

2.3. INS reaction regime

Approximately 20 g of catalyst was loaded into the reactor between quartz wool plugs. The sample was reduced for 2 h at 550 °C before either isolation and removal, or dry-reforming reaction at the same temperature for 100 min. The reduction was carried out under 140 ml min^{-1} H_2, whilst the reaction flow rates were 70 ml min^{-1} of both CO_2 and CH_4. 1250 ml min^{-1} He was used as a diluent in both cases. All gases were provided by CK gases and were used without further purification. These arrangements corresponded to the reactor operating at a GHSV of 4170 $cm^3/(g_{cat}\ h)$ and a mean contact time of 5.3×10^{-3} min. It is noted that the space velocity is lower for the INS measurements compared to those utilised in the micro-reactor studies. This is a constraint of working with such a large catalyst mass that is required for the INS measurements.

The mass spectrometer showed methane conversions and reaction selectivities comparable to those observed in the micro-reactor studies. After a fixed reaction time (100 min), heating and flow of reacting gases was stopped and the reactor allowed to cool in the presence of flowing helium. This arrangement approximates to the 'quench' approach previously adopted by Goodman and co-workers [23,24]. Once the sample temperature was at ambient, the catalyst sample was transferred to an indium-sealed gas tight aluminium sample can inside an argon-filled glove box (MBraun UniLab MB-20-G, $[H_2O] < 1$ ppm, $[O_2] < 2$ ppm). This cell was then transferred to the INS spectrometer. After these measurements, any radioactivity was allowed to decay to a safe level before the catalysts were recovered and used in subsequent IR and TPO experiments. In order to evaluate the role of the support material in the resulting chemical transformations, a series of blank measurements were undertaken where a sample of alumina was reduced in exactly the same way as with the Ni/Al_2O_3 sample, and subsequently reacted for 180 min.

2.4. Post-reaction characterisation

INS measurements were carried out on the TOSCA spectrometer [25] at the ISIS Facility, Rutherford Appleton Laboratory. TOSCA is an indirect geometry instrument with graphite crystal analysers. The samples were cooled to *ca.* 30 K before data acquisition to minimise the Debye–Waller factor and collection times were of the order of 16 h.

Transmission infrared measurements utilising the recovered catalyst were carried out on a Bruker Vertex 70 using discs pressed without diluent in a 13 mm die under 10 tonnes pressure. Spectra were recorded using a high D^* mercury cadmium telluride detector at 4 cm^{-1} resolution. Temperature-programmed oxidation (TPO) of the deposited material was carried out on custom-built apparatus using a quadrupole mass spectrometer (Leda Mass Gas Analyser, LM22). Approximately 30 mg of catalyst was placed between quartz wool plugs in a 1/4-in. O.D. stainless steel tube within a programmable oven (Neytech 25PAF). The sample was heated at 10 °C min^{-1} to 900 °C under a 40 ml min^{-1} flow of 5% O_2 in He. Quantification of the extent of carbon present in the spent catalyst was made with reference to calibration plots prepared using the oxidation of graphite as well as the thermal decomposition of calcium carbonate.

3. Results

3.1. Micro-reactor reaction measurements

The catalyst was first tested for its reforming performance using a conventional micro-reactor arrangement. A 1:1 mixture of methane and carbon dioxide was selected as it will support reforming whilst also exhibiting carbon laydown processes. It is these carbon deposition processes that this study aims to concentrate on. Fig. 1 shows the TPR profile for the Ni/Al_2O_3 catalyst. A broad feature centred at 440 °C is seen, which is associated with the reduction of NiO to form metallic nickel (Ni^0). Both the hydrogen and water signals return to baseline levels at 510–520 °C, indicating that the catalyst is fully reduced after heating to temperatures of *ca.* 500 °C in the presence of flowing hydrogen.

Fig. 2 shows a TPRxn plot for the activated catalyst. No reaction is seen until an onset temperature of 450 °C, where upon consumption of the CH_4 and CO_2 reagents becomes dramatically apparent. This results in the formation of equimolar quantities of CO and H_2, indicating the 'dry' reforming process (Eq. (1)) to be active:

$$CH_4 + CO_2 \rightarrow 2CO + 2H_2 \quad (1)$$

The CO and H_2, signals rise concomitantly and saturate at about 800 °C. The presence of water is also detected during the initial stages of reaction, as evidenced by a broad distribution between 450 and 800 °C. This is attributed to the reverse water gas shift reaction (Eq. (2)) being active within this region:

$$H_2 + CO_2 \rightarrow CO + H_2O \quad (2)$$

where hydrogen product from the 'dry' reforming reaction is reacting with the reactant carbon dioxide.

A plot of methane conversion as a function of temperature is shown in Fig. 3(a), with reaction commencing abruptly at 440 °C and complete conversion evident at temperatures above 780 °C. Fig. 3(b) displays the H_2:CO ratio over the temperature range studied. After some variability about the 'light-off' temperature of 440 °C, a H_2:CO ratio of approximately unity is maintained, which gradually decreases with increasing temperature.

INS experiments on a working catalyst are a non-trivial matter [21]. One factor that has to be considered is compatibility of reaction cells with the INS measurement. To this end, we favoured the use of a separate reactor that could accommodate the large mass of sample required to produce a measurable INS spectrum. We also wished to run under isothermal conditions and to analyse the sample at the end of a period of sustained formation of

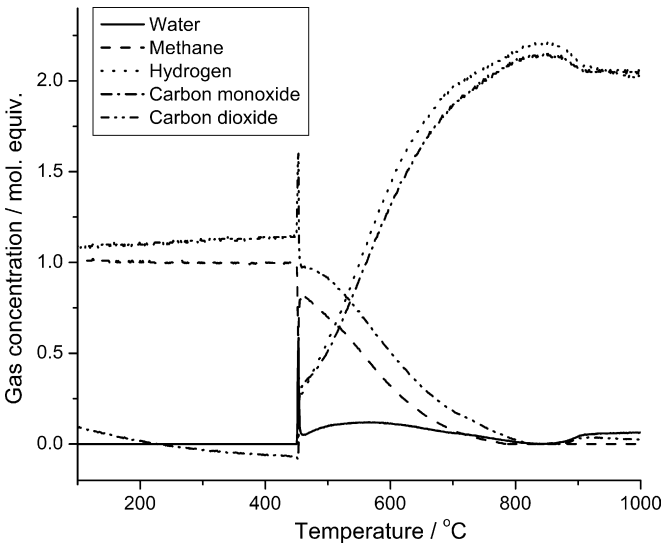

Fig. 2. Normalised product and reactant concentrations for dry-reforming reaction under temperature-programmed heating (5 °C min^{-1}) for 26% Ni/Al_2O_3 catalyst.

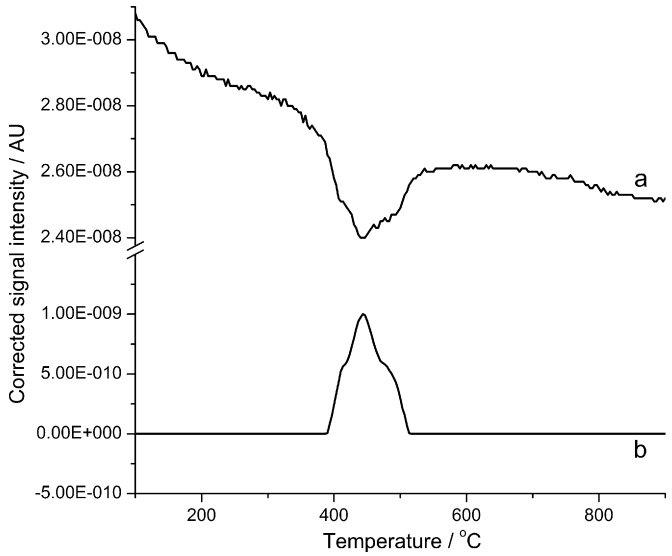

Fig. 1. (a) Hydrogen uptake and (b) water production in temperature-programmed reduction (TPR) profile for 26% Ni/Al_2O_3 catalyst heated at 5 °C min^{-1}.

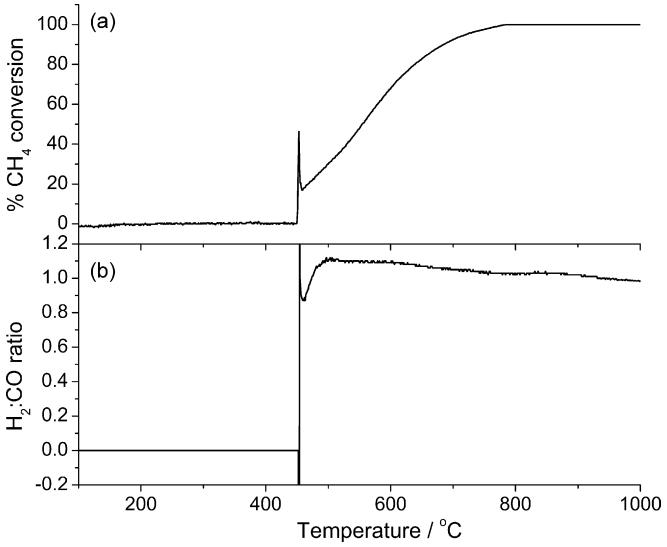

Fig. 3. Variation of (a) methane conversion and (b) H_2:CO ratio under temperature-programmed reaction on 26% Ni/Al_2O_3 catalyst heated at 5 °C min^{-1} as shown in Fig. 2.

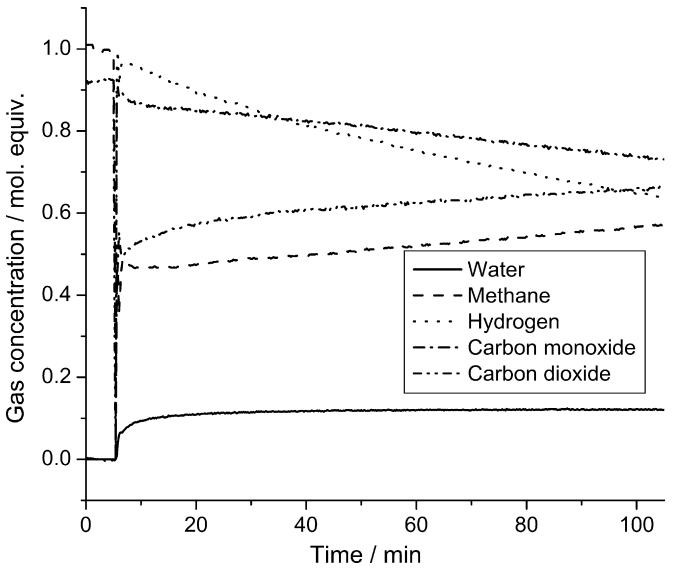

Fig. 4. Normalised product and reactant concentrations for dry-reforming reaction maintained at 550 °C for 100 min over 26% Ni/Al_2O_3 catalyst.

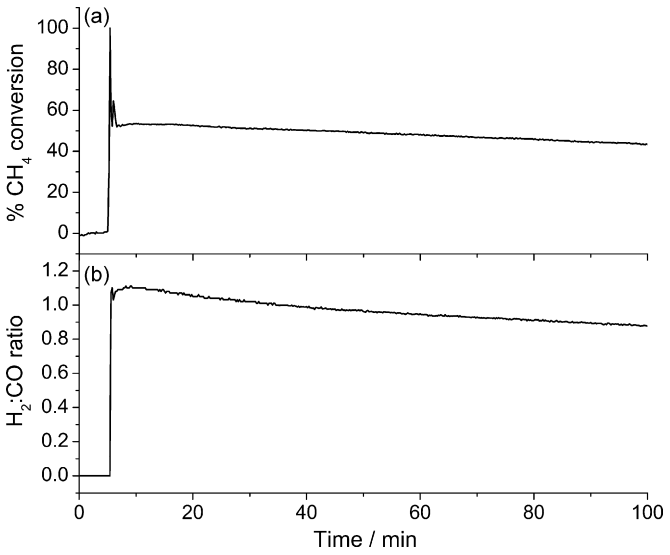

Fig. 5. (a) Methane conversion and (b) ratio of H_2:CO under isothermal reaction maintained at 550 °C for 100 min over 26% Ni/Al_2O_3 catalyst as shown in Fig. 4.

reaction products. The afore-mentioned 'quench' approach [23,24] was selected as providing the preferred means of achieving these aims. Given the temperature constraints of the valves associated with the stainless steel reactor, a reaction temperature of 550 °C was selected. With reference to Fig. 3(a), this corresponds to a respectable methane conversion of *ca.* 46% and is within the range reported by other workers. For instance, for this reaction system Zhu et al. [26] and Yashimi et al. [2], respectively, report conversions of 75% at 750 °C with a GHSV of 60000 $cm^3/(g_{cat}\ h)$ and 72% at 800 °C with a GHSV of 48000 $cm^3/(g_{cat}\ h)$, whereas Verykios et al restrict their reaction parameters to retain methane conversion of *c.* 15% at 500 °C for nickel supported on γ-Al_2O_3 [3].

Fig. 4 presents an isothermal run for the carbon dioxide reforming of methane with the micro-reactor maintained at 550 °C. Flow of the reactants is established over a bypass before switching through the catalyst bed after 5 min. This accounts for the rapid change in the data at this point. The profiles indicate that the system is progressively working towards a steady-state operation after an initial conditioning period, although the product streams are not fully stabilised within the 100 min time on stream presented in Fig. 4. Consistent with the TPRxn data (Fig. 2), the reverse water gas shift reaction is also active during the isothermal run. Fig. 5(a) shows the associated methane conversion plot, which declines from an initial conversion of 52–43% over a period of 100 min. This reduction is attributed to carbon laydown processes, which constitute side reactions to the mainstream reforming process (Eq. (1)) that progressively reduce catalyst activity. The H_2:CO ratio is presented in Fig. 5(b) and, in contrast to the temperature-programmed case (Fig. 3(b)), indicates the H_2:CO ratio to progressively decrease below unity for reaction times beyond 40 min as a function on time on stream. This indicates that the hydrogen yield is falling below that seen for CO. Two scenarios could account for this observable: either hydrogen is being retained at the catalyst surface or, alternatively, the extra hydrogen consumption is associated with the reverse water gas shift activity (Eq. (2)). This matter will be revisited upon consideration of the INS spectra (Section 3.2).

After 100 min on stream (Fig. 4), a TPO spectrum for the catalyst was obtained, presented in Fig. 6(a), that is characterised by an intense feature centred at 570 °C, the distribution of which is slightly skewed to low temperature. The integrated area of this feature corresponds to 4.7×10^{22} C atoms $g^{-1}_{(cat)}$, which represents a carbon loading of 49 wt%. Thus, during the course of reaction sequence displayed in Fig. 4, the catalyst has retained significant quantities of carbon (coke). This is an interesting outcome, for despite the catalyst facilitating deposition of carbon over the reaction period, it is noted that Figs. 4 and 5 show the catalyst to be still successfully reforming methane to a reasonable extent. Given the quantity of the retained carbon, it is thought that a sizeable proportion must be residing on the support material as otherwise, one would expect the metal sites to become completely deactivated, which as Figs. 4 and 5 indicate, is clearly not the case. Moreover, the TPO profile (Fig. 6(a)) additionally provides information on the nature of the carbon, with the relatively low temperature band-head clearly demonstrating an absence of graphite within the reaction system. This is consistent with the maintenance of a large degree of the initial catalyst activity and is suggestive of the presence of amorphous carbon.

3.2. Inelastic neutron scattering

INS spectra of the samples were recorded (a) with the catalyst reduced in hydrogen prior to reaction and (b) after 'dry' reform-

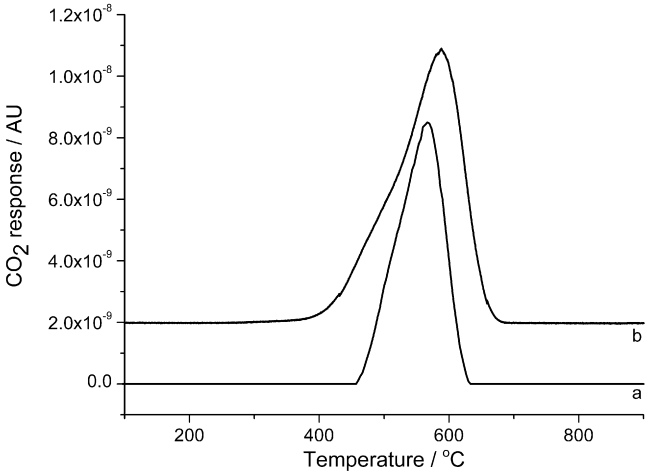

Fig. 6. Temperature-programmed oxidation (TPO) after (a) isothermal reaction maintained at 550 °C for 100 min over 26% Ni/Al_2O_3 catalyst in micro-reactor as shown in Fig. 5 and (b) isothermal reaction maintained at 550 °C for 120 min over 26% Ni/Al_2O_3 catalyst in INS reactor (Fig. 7(b)).

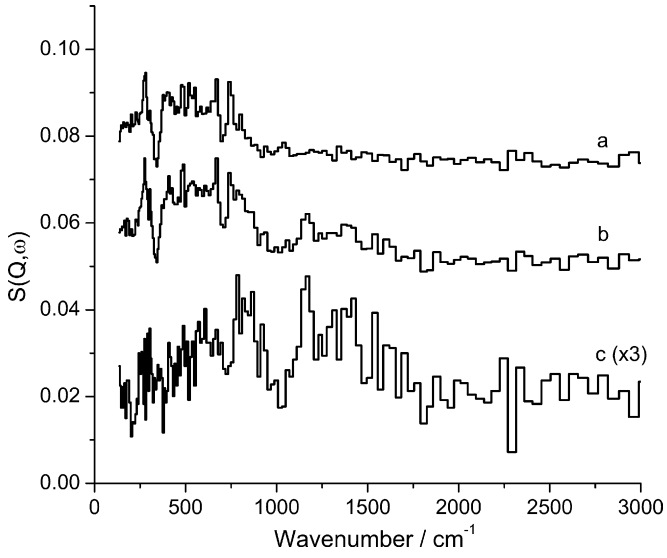

Fig. 7. INS spectra of 26% Ni/Al_2O_3 catalyst sample after (a) reduction for 120 min at 550 °C and (b) subsequent 100 min dry-reforming at 550 °C. The subtracted spectrum [(b) – (a)] is presented in (c), i.e. where the spectrum of the reduced catalyst has been subtracted from the spectrum of the reacted sample.

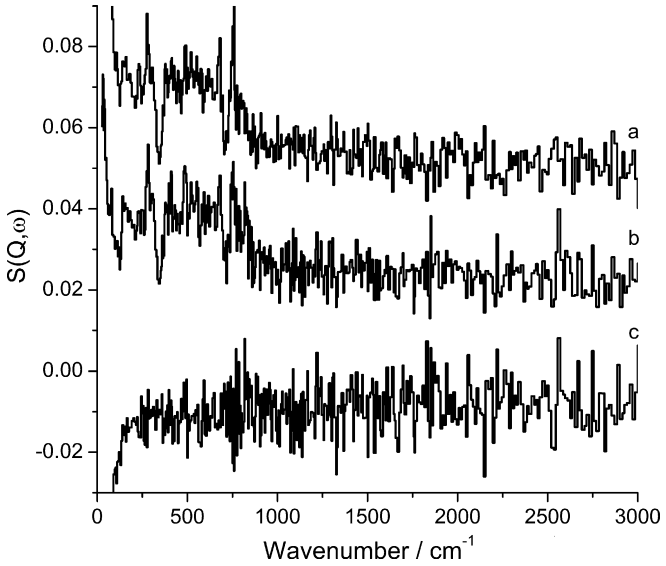

Fig. 8. INS spectra of Al_2O_3 support material after (a) reduction for 120 min at 550 °C and (b) subsequent exposure to co-feeding CH_4 and CO_2 at 550 °C for 180 min. The subtracted spectrum [(b) – (a)] is presented in (c), i.e. where the spectrum of the activated alumina has been subtracted from the spectrum of the alumina exposed to dry-reforming conditions.

ing for 100 min. Both spectra are shown in Fig. 7 and display an unexpectedly low signal, indicating a very small quantity of hydrogen in the sample. The dominant features below 1000 cm^{-1} are seen in both reduced and reacted samples and are therefore due to the catalyst. To eliminate these common features and elucidate the difference between samples due to the deposited material, subtraction of the reacted-reduced spectra was undertaken, Fig. 7(c). The resulting spectrum shows similar features to carbon blacks reported previously using INS as a vibrational probe [27,28], for example the industrial grade carbon black material N234 [17]. The dip in intensity at 1000 cm^{-1} suggests sizeable polycyclic aromatic species are present [17]. Spectral features can be tentatively assigned as C–C torsion (273 cm^{-1}), C–H out-of-plane bend (824 cm^{-1}) and C–H in-plane bend (1157 cm^{-1}). The spectrum of graphite has previously been recorded on the precursor instrument TFXA and contrasts significantly with Fig. 7(c) [29]. Although of low intensity, the data exclude the presence of well ordered graphite to any significant degree, which agrees with the modest deactivation seen over the course of reaction (Figs. 4 and 5) as well as the TPO profile (Fig. 6(a)).

Fig. 7(c) shows no contribution from chemisorbed hydrogen [21]. Rather, it is interpreted as corresponding to a form of amorphous hydrogenated carbon with a surprisingly low hydrogen content. Using the TOSCA spectrometer, Albers et al. have correlated scattering intensity for carbonaceous materials with hydrogen content [17]. Comparing the spectral intensity inherent in Fig. 7, it is evident that the hydrogen content in the overlayer is <1000 ppm. Indeed, this is indicative of how efficient these catalysts are at cycling hydrogen. This analysis then enables rationalisation of an issue identified in the micro-reactor studies (Section 3.1), namely how the hydrogen is being partitioned during reaction. Given the weak neutron scattering intensity apparent in Fig. 7, then the possibility that hydrogen is being incorporated in to the carbon matrix due to any significant degree must be discounted. Instead the sub-unity values for the H_2:CO ratio (Fig. 5(b)) must be related to the reverse water gas shift activity apparent in Fig. 4.

For comparison purposes, the INS spectra of the activated alumina is shown in Fig. 8(a). A peak at 280 cm^{-1} is assigned to the out-of plane hydroxyl deformation of alumina, whereas the in-plane hydroxyl deformation is seen at 750 cm^{-1}. These features are evident in the Ni/Al_2O_3 spectra (Fig. 7), indicating the support material to be making a significant contribution to the INS spectrum of the un-reacted catalyst. The alumina was then exposed to the same 'dry' reforming conditions as experienced by the Ni/Al_2O_3 catalyst, with the spectrum presented in Fig. 8(b). The in-line mass spectrometer indicated that no methane conversion occurred during this exercise. Given that Fig. 8(b) so closely resembles Fig. 8(a) and that no features are apparent upon subtraction (Fig. 8(c)), this indicates that the favourable chemistry seen in Fig. 4 is metal-mediated, with no direct role for the support material.

3.3. Post-reaction analysis of INS samples

3.3.1. Temperature-programmed oxidation

The TPO spectrum for the Ni/Al_2O_3 catalyst that yielded the INS spectrum shown in Fig. 7(b) is presented in Fig. 6(b). It is characterised by an intense feature centred at 600 °C, which exhibits a low temperature shoulder at *ca.* 500 °C. Comparing this INS sample with Fig. 6(a) indicates some differences between the two samples. The micro-reactor sample (Fig. 6(a)) is typified by onset, peak and maximum temperatures of 450, 570 and 630 °C, respectively; whereas the larger reactor sample displays values of 400, 600 and 680 °C. Thus the INS sample displays a wider profile but, nevertheless, the two TPO spectra are broadly similar and indicate that the catalyst surface post-reaction in the micro-reactor studies is comparable to that seen when the reaction is scaled up by a factor of *ca.* 1000 for the INS measurements. Integration of the peak in Fig. 6(b) corresponds to 6.2×10^{21} C atoms $g^{-1}_{(spent\ cat)}$, which corresponds to the catalyst extracted from INS reactor having a carbon loading of 12 wt%.

Unfortunately, it is not possible to make a direct comparison between this value and the level of carbon seen with the micro-reactor set-up (carbon loading = 49%). Whereas the latter value is an *in situ* TPO measurement that is normalised to the mass of pre-reduced catalyst, the post-reaction INS sample is an *ex situ* TPO measurement that is normalised to the mass of catalyst post-reaction. Thus, changes in the density and form of the catalyst as a consequence of activation and reaction complicate direct comparisons between the two samples. Such issues highlight the benefit that a full *in situ*/Operando approach to investigating this challeng-

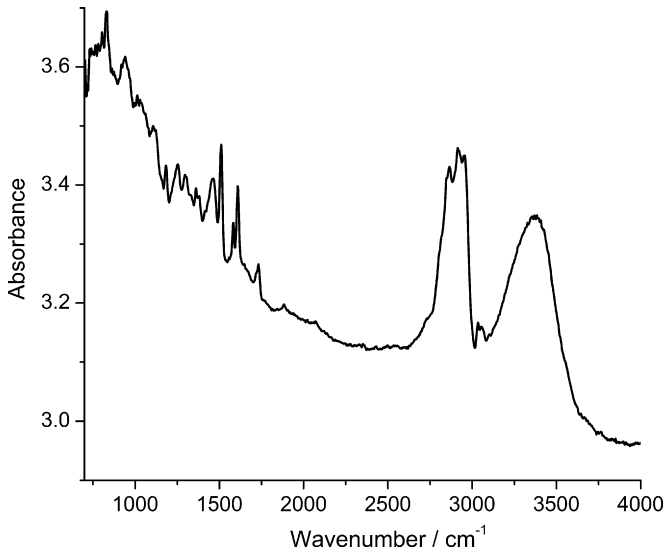

Fig. 9. Transmission infrared spectrum of 26% Ni/Al_2O_3 catalyst sample after reaction for 100 min at 550 °C.

ing reaction system would allow. So, despite presenting similar TPO profiles (Fig. 6) it appears that the carbon laydown seen for the micro-reactor significantly exceeds that seen for the larger INS reactor. Replicate TPO runs on the INS sample show the 12% carbon laydown value to be representative of the full catalyst charge. It is possible that the disparity between the coke values for the two reactor configurations reflect differences in the contact times, with the longer contact time of the INS set-up seemingly favouring CO production over the carbon deposition process.

3.3.2. Infrared spectroscopy

The infrared spectrum of the catalyst recorded post-reaction is displayed in Fig. 9.

Table 1
A description of features seen in the infrared spectrum of the Ni/Al_2O_3 catalyst post-reaction (Fig. 9).

ν/cm^{-1}	Assignment
3373	ν(OH)
3057	$\nu_{asym}(CH_2)$ alkene ν(CH) aromatic
3036	ν(CH) alkene ν(CH) aromatic
2955	$\nu_{asym}(CH_3)$ $\nu_{sym}(CH_2)$ alkene
2917	$\nu_{asym}(CH_2)$ alkane
2866	$\nu_{sym}(CH_3)$
2847	$\nu_{sym}(CH_2)$ alkane
1732	ν(CO) aliphatic ketone
1609	δ(OH) $water_{ads}$ Skeletal aromatic ring mode
1583	ν_{sym} $(CO_3)^{2-}$ organic Skeletal aromatic ring mode
1510	$\nu(CO_3)^{2-}$ Skeletal aromatic ring mode
1457	$\nu(CO_3)^{2-}$ Alkene CH_2 scissor Asym methyl deform
1415	$\nu_{sym}(CO_3)^{2-}$ inorganic Alkene CH_2 scissor
1361	Methyl sym bend
1298	Alkene CH rock

The spectrum displays the following features; a broad hydroxyl stretching peak at 3373 cm^{-1}, a complex CH stretching region including saturated and unsaturated materials, a carbonyl group peak at 1732 cm^{-1} and a dense collection of peaks in the fingerprint region. Major peaks and their suggested assignments are shown in Table 1.

The hydroxyl peak can be ascribed to the presence of surface hydroxyls on the alumina support and adsorbed water. A small CH stretching peak displaying maxima at 3036 and 3057 cm^{-1} can be attributed to either aromatic or alkene groups. Evidence for saturated hydrocarbons can be seen in the more sizeable peak centred around 2900 cm^{-1}. The fine structure of this region demonstrates a variety of species although a definitive assignment has not been attempted. A small peak is seen at 1732 cm^{-1}, which is attributed to a carbonyl stretching mode. The frequency could represent an aliphatic ketone [30], which is consistent with the large aliphatic contribution to the C–H stretching region. The peak at 1610 cm^{-1} is due to the presence of adsorbed water, which is likely to have been absorbed during the process of the infrared sample handling and measurement process. Peaks below this may be due to either hydrocarbon deformations (1457, 1415, 1381, 1361 and 1298 cm^{-1}), skeletal aromatic ring vibrations (1583 and 1510 cm^{-1}) or carbonate species (1583, 1510, 1457 and 1415 cm^{-1}); the latter grouping most likely associated with the alumina support material. The peak at 1583 cm^{-1} has been previously labelled the "coke band" and is assigned to C=C stretching vibrations of carbonaceous deposits [31]. From deductions outlined above, the nature of the coke in this instance is thought to be non-graphitic. Catalytic activity is expected to be quenched by the presence of graphite, therefore its absence at the catalyst surface is consistent with the generally high activity apparent in the reaction test data (Figs. 4 and 5). Linking these concepts with the INS and TPO measurements, the presence of the 1583 cm^{-1} band is therefore attributed to amorphous carbon in this instance. It is recognised that the phase diagram of the retained carbonaceous deposits is complex and can encompass a

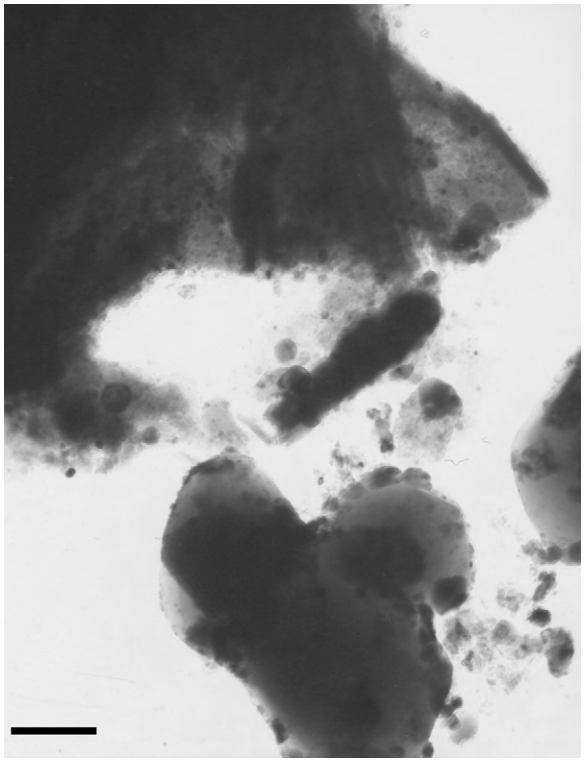

Fig. 10. Transmission electron micrograph of 26% Ni/Al_2O_3 catalyst sample after reaction for 100 min at 550 °C.

variety of carbonaceous materials (hydrocarbonaceous overlayers, amorphous carbon, microcrystalline graphite, extended graphite sheets, etc.) with amorphous carbon being particularly poorly defined. Nevertheless, within the limitations of this definition, this is thought to be the dominant species present at the catalyst surface in this instance.

3.3.3. Transmission electron microscopy

Fig. 10 displays a typical electron micrograph of the catalyst after reaction in the INS cell. Dark spherical metal particles of varying dimensions are contrasted against the more transparent alumina support material. Previous studies on the reforming of methane over supported nickel catalysts have identified filamentous carbon growth centred from the metal crystallites [1]. No such structures are evident in Fig. 10, consistent with the carbon laydown processes yielding a coke residue that corresponds to amorphous carbon.

4. Discussion

The reaction data show that there is a deposition of carbon over the short reaction period studied. The INS data indicate that very little hydrogen is retained in the coke formed during this reaction sequence. Thus, the material deposited is almost completely composed of carbon. Temperature-programmed oxidation of the coke shows carbon deposits which are oxidised across a wide temperature range consistent with the presence of amorphous carbon [32]. The breadth of the desorption feature is thought to reflect the presence of domains of varying size. The ν(C–H) stretching modes in the infrared spectrum indicate that the majority of the bound hydrogen is associated with aliphatic moieties. The infrared spectrum also demonstrates the presence of oxygen in the carbon as a carbonyl group, although at a much lower concentration than the hydrogenous modes. Bartholomew [5] describes the mechanisms of coke formation in steam reforming as either reactions between atomic C_α to form pure carbons, or CH_x fragments to form hydrocarbon cokes which may be dehydrogenated to form pure carbons. Both of these methods will be present for dry-reforming, but the incorporation of small quantities of oxygen in to the matrix demonstrates there is also a role for CO or CO_2 in the coke formation process during 'dry'-reforming conditions.

This multi-technique study has demonstrated how efficient these catalysts are at cycling hydrogen. Despite continual carbon laydown that forms an amorphous carbon overlayer, which ultimately will impede activity (not particularly evident in this work), there is very little incorporation of hydrogen in to the carbonaceous network. The infrared measurements indicate the presence of carbon-hydrogen plus a minor contribution from carbon-oxygen species, both predominantly present in an aliphatic environment. It is thought that these functional units are present as terminations of phase boundaries of extended carbonaceous networks.

It is intriguing to speculate how the catalyst actually operates. The fact that the alumina showed no activity and that the INS spectrum showed no change after exposure to the gas mixtures at 550 °C (Fig. 8) indicate this material not to be responsible for initiating reaction. Both the micro-reactor and INS reactor measurements indicated nearly steady-state operation at 550 °C despite considerable carbon laydown (4.7×10^{22} C atoms $g^{-1}_{(\text{pre-reaction cat})}$ and 6.2×10^{21} C atoms $g^{-1}_{(\text{post-reaction cat})}$ for the micro-reactor and INS reactions, respectively). This outcome indicates that the deposited carbon is not significantly impeding reaction. The assignment to amorphous carbon containing a surprisingly small quantity of hydrocarbonaceous material (Fig. 7) is consistent with the fact that the carbon is porous to reactants and products, as must be the case for the sustained product formation seen in both cases. Given that hydrogen exchange is pivotal in the methane reforming process (Eq. (1)), it is possible that hydrogen is retained about the metal/carbon interface, where the methane reforming process is thought to actually take place. Further work is focussing on investigating this hypothesis.

Finally, the procedure outlined here has shown how INS can be used to provide vibrational spectroscopic information in the 50–2000 cm^{-1} spectral region of the spectrum. Moreover, the technique additionally provides valuable information on the concentration of hydrogen present at the catalyst surface. This information is most useful in developing models for how catalysts facilitate favourable molecular transformations at the gas–solid interface.

Acknowledgements

The authors would like to thank the EPSRC for overall funding (Grant EP/E028861/1) and the Rutherford Appleton Laboratory for access to the neutron spectrometer.

References

[1] M.C.J. Bradford, A.M. Vannice, Appl. Catal. A: Gen. 142 (1996) 73.
[2] Z. Hou, O. Yokota, T. Tanaka, T. Yashimi, Catal. Lett. 89 (2003) 121.
[3] Z.L. Zhang, X.E. Verykios, Catal. Today 21 (1994) 589.
[4] J.R. Rostrup-Nielsen, J.-H. Bak Hansen, J. Catal. 144 (1993) 38.
[5] C.H. Bartholomew, Catal. Rev. 24 (1982) 67.
[6] D.L. Trimm, Catal. Today 37 (1997) 233.
[7] S. Helveg, C. López-Cartes, J. Sehested, P.L. Hansen, B.S. Clausen, J.R. Rostrup-Nielsen, F. Abild-Pedersen, J.K. Nørskov, Nature 427 (2004) 426.
[8] N. Jeong, J. Lee, J. Catal. 260 (2008) 217.
[9] P. Albers, S. Bösing, G. Prescher, K. Seibold, D.K. Ross, S.F. Parker, Appl. Catal. A: Gen. 187 (1999) 233.
[10] Y.T. Chua, P.C. Stair, J. Catal. 213 (2003) 39.
[11] J. Datka, Z. Sarbak, R.P. Eischens, J. Catal. 145 (1994) 544.
[12] D.G. Blackmond, J.G. Goodwin Jr., J.E. Lister, J. Catal. 78 (1982) 247.
[13] P. Albers, H. Angert, G. Prescher, K. Seibold, S.F. Parker, Chem. Commun. 17 (1999) 1619.
[14] A.R. McInroy, D.T. Lundie, J.M. Winfield, C.C. Dudman, P. Jones, S.F. Parker, J.W. Taylor, D. Lennon, Phys. Chem. Chem. Phys. 7 (2005) 3093.
[15] D. Lennon, J. McNamara, J.R. Philips, R.M. Ibberson, S.F. Parker, Phys. Chem. Chem. Phys. 2 (2000) 4447.
[16] P. Albers, J. Pietsch, S.F. Parker, J. Mol. Catal. A: Chem. 173 (2001) 275.
[17] P.W. Albers, J. Pietsch, J. Krauter, S.F. Parker, Phys. Chem. Chem. Phys. 5 (2003) 1941.
[18] P.W. Albers, S. Bösing, H. Lansink Rotgerink, D.K. Ross, S.F. Parker, Carbon 40 (2002) 1549.
[19] A.R. McInroy, D.T. Lundie, J.M. Winfield, C.C. Dudman, P. Jones, D. Lennon, Langmuir 21 (2005) 11092.
[20] J.M. Ginsberg, J. Piña, T. El Solh, H. de Lasa, Ind. Eng. Chem. Res. 44 (2005) 4846.
[21] P.C.H. Mitchell, S.F. Parker, A.J. Ramirez-Cuesta, J. Tomkinson, Vibrational Spectroscopy with Neutrons, World Scientific, Singapore, 2005, p. 285.
[22] C. Finnerty, R. Cunningham, R. Ormerod, Catal. Lett. 66 (2000) 221.
[23] S. Chinta, T.V. Choudhary, L.L. Daemen, J. Eckert, W.D. Goodman, Angew. Chem. Int. Ed. 41 (2002) 144.
[24] C. Sivadinarayana, T.V. Choudhary, L.L. Daemen, J. Eckert, D.W. Goodman, J. Am. Chem. Soc. 126 (2004) 38.
[25] D. Colognesi, M. Celli, F. Cilloco, R.J. Newport, S.F. Parker, V. Rossi-Albertini, F. Sacchetti, J. Tomkinson, M. Zoppi, Appl. Phys. A 74 (2002) S64.
[26] X. Zhu, P. Huo, Y. Zhang, D. Cheng, C. Liu, Appl. Catal. B: Environ. 81 (2008) 132.
[27] P. Albers, G. Prescher, K. Siebold, D.K. Ross, F. Fillaux, Carbon 34 (1996) 903.
[28] P. Albers, Carbon 37 (1999) 437.
[29] J.K. Walters, R.J. Newport, S.F. Parker, W.S. Howells, J. Phys. Condens. Matter 7 (1995) 10059.
[30] D. Lin-Vien, N.B. Colthup, W.G. Fateley, J.G. Grasselli, The Handbook of Infrared and Raman Characteristic Frequencies of Organic Molecules, Academic Press, San Diego, 1991, p. 479.
[31] D. Eisenbach, E. Gallei, J. Catal. 56 (1979) 377.
[32] P. Wang, E. Tanabe, K. Ito, J. Jia, H. Morioka, T. Shishido, K. Takehira, Appl. Catal. A: Gen. 231 (2002) 35.